PAPER NUMBER 61-LUB-11

AN ASME PUBLICATION

Experimental Investigation of Oilfilm Behavior in Short Journal Bearings[1]

BORIS AUKSMANN

Research Engineer,
Ingersoll-Rand Company,
Phillipsburg, N. J.
Assoc. Mem. ASME

A brief description is given of the apparatus designed ... experimental investigation of oil-film behavior in short full journal bearings of the circumferential feed-groove type. Experimental pressure distributions for the complete bearing are presented in graphical form for four typical test runs. Comparison is made with the theoretical solution developed by F. W. Ocvirk for two cases where cavitation in the test bearing was completely suppressed. Agreement with the theory was good for pressurized bearing operated at a low axial pressure gradient. Visual observations of the cavitation phenomena are discussed with references to the photographs.

1 This paper is based on the investigation carried out by the author in partial fulfillment for the degree of Mechanical Engineer, California Institute of Technology, Pasadena, Calif.

Contributed by the Lubrication Division of The American Society of Mechanical Engineers for presentation at the ASME-ASLE Lubrication Conference, Chicago, Ill., October 17-19, 1961. Manuscript received at ASME Headquarters, July 11, 1961.

Written discussion on this paper will be accepted up to November 30, 1961

Copies will be available until August 1, 1962

THE AMERICAN SOCIETY OF MECHANICAL ENGINEERS
345 East 47th Street, New York 17, N. Y.

Experimental Investigation of Oilfilm Behavior in Short Journal Bearings

BORIS AUKSMANN

NOMENCLATURE

C_R = radial clearance, in.
d = journal diameter, in.
e = eccentricity of journal and bearing axes, in.
h = local fluid film thickness, in.
ℓ = bearing length, in.
n = eccentricity ratio or attitude = e/C_R
P = applied load, lb
P_x, P_y = components of applied load parallel and normal to line of centers of journal and bearing, lb
P_s = supply plenum pressure, psi
P_D = discharge plenum pressure, psi
p = local fluid film pressure, psi
U = surface speed of journal, ips
x, y, z = co-ordinates
θ = angle measured from maximum film thickness in the direction of rotation, deg
μ = absolute viscosity of lubricant centipoises/$(6.9\text{x}10^6)$
Φ = attitude angle between load line and line of centers of journal and bearing, deg

INTRODUCTION

Several analytical expressions have been developed for pressure distribution in short journal bearings. Most of these are based on approximate solutions of Reynolds' equation:

$$\frac{\partial}{\partial x}\left(h^3 \frac{\partial p}{\partial x}\right) + \frac{\partial}{\partial z}\left(h^3 \frac{\partial p}{\partial z}\right) = 6\mu U \frac{\partial h}{\partial x} \qquad (1)$$

by neglecting the first term on the left side of the equation. Experimental data and theory have been compared by several investigators (1, 2, 3)[1] with various degrees of agreement; however, the negative pressure[2] region predicted by theoretical solutions has been omitted in these comparisons. Usually the assumption is made that cavitation breaks up the diverging oil film and relieves negative pressures at the vapor-pressure level of the lubricant (3), and that the load is supported by the positive-pressure region only. Thus, if the assumption about cavitation is correct, load-carrying capacity of a journal bearing could be doubled by suppressing the cavitation. However, a theoretical solution by Wannier (4), offers an alternative pressure-relief mechanism through reverse flow in the divergent film region, giving no load-capacity increase if the bearing is pressurized.

This experimental investigation was conducted to provide data for comparison with theoretical solutions, particularly for the negative-pressure regions, and to observe cavitation phenomena visually. Pressures were measured over the entire circumference in a short journal bearing with a circumferential feed groove; tests were made mostly at elevated datum pressures and/or with high axial gradients so that cavitation would be suppressed or limited to small regions farthest from the feed groove.

APPARATUS

For visual observation of the oil film, the apparatus was designed around a transparent test bearing. This material limitation necessitated use of light lubricants so that pressures developed in the oil film at high eccentricity ratios would not cause bearing distortion or cracking.

The test-bearing arrangement, section view, and piping diagram of the apparatus are shown in Figs. 1, 2 and 3, respectively. A 2-in-diam precision-ground shaft is mounted on opposed precision roller bearings inside a floating-disk assembly. The latter is supported between two hydraulic pads permitting the shaft to take up its equilibrium position inside the test bearing without any frictional effects and with a runout of less than 0.00005 in. The test bearing is essentially one half of a bearing with circumferential feed groove in the middle; the supply plenum chamber takes the place of the feed groove and a second plenum chamber is added for the discharge control. The test bearing is held rigidly between two rings which also serve as plenum chambers for lubricant circulation, form the manifolds for pressure tap connections, contain lip seals and affix the entire bearing assembly to the supporting column. The load is applied to the test shaft by weights hanging on the wire connected to the floating disk through a sliding ring allowing variation of

[1] Underlined numbers in parentheses designate References at the end of the paper.

[2] Negative pressure with respect to a datum which is defined as the average pressure level for the particular distribution curve.

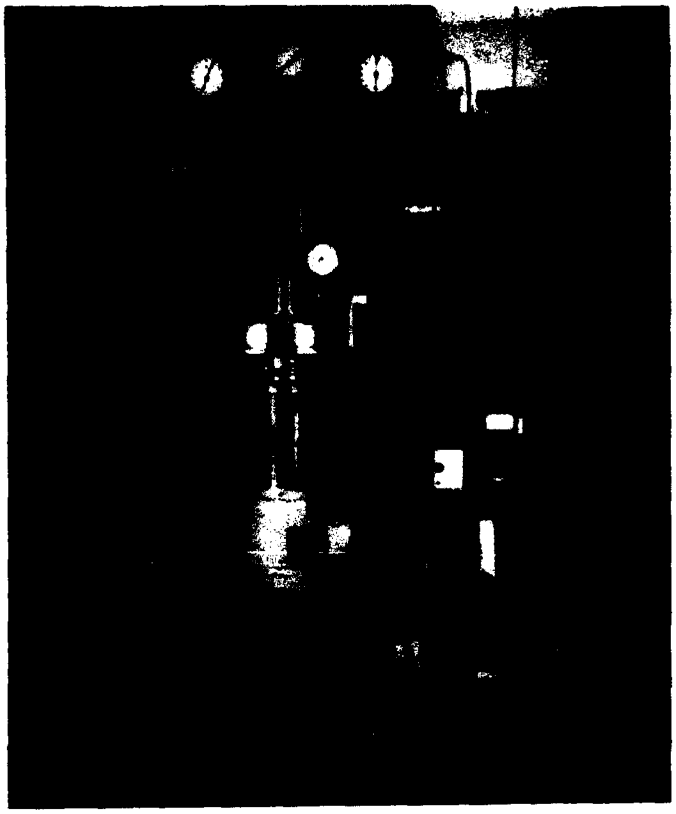

Fig. 1(a) Test-bearing setup with instrumentation

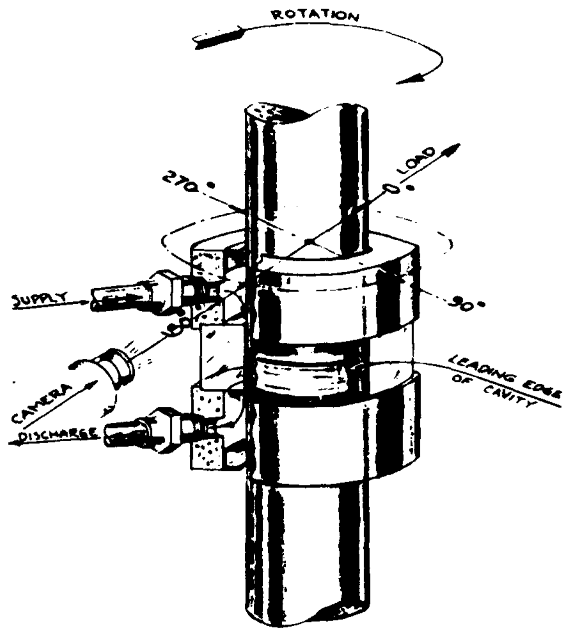

Fig. 1(b) Test-bearing arrangement

the load direction over an angle of 200 deg. With two diametrically opposite sets of pressure taps complete circumferential pressure distribution can be measured with 20-deg overlaps at pressure-tap locations.

Eccentricity of the journal was measured by two perpendicularly oriented dial gages (of 0.0001 in. per division sensitivity) riding directly on the top end of the test shaft. Test-bearing supply and discharge pressures were measured with calibrated bourdon gages; pressures in the test-bearing oil film were measured by a pressure transducer energized from a 1000-cps constant voltage a-c source and a vacuum-tube voltmeter. Deaerated diesel fuel was used as the lubricant in all test runs.

PRESSURE MEASUREMENTS

For pressure-distribution measurements, the 2.0000-in-OD shaft was used in combination with a lapped brass bearing of 2.0041 in. average ID and 1 in. long. Radial clearance variations due to bearing bore inaccuracies were determined to be less than 5 per cent of the average C_R-value of 0.00205 in. The bearing was drilled for six 0.020-in-diam pressure taps located in two sets 180 deg apart; each set having taps at one quarter, one half and three quarters of the axial length.

Typical pressure distributions obtained are shown in Figs.4 to 7, together with variables for each run. The stated attitude angle Φ and eccentricity ratio n-values are averages based on displacement measurements for three different load directions. The viscosity and temperature values are for the conditions in the lubricant supply reservoir. The maximum speed variation for any one run is estimated at $\pm$ 0.5 per cent.

It is of interest to compare test data with the theoretical pressure distribution of Ocvirk's solution (1). Of course, comparison with theory is meaningful only for the cases without cavitation since the extent of the cavity and pressure within the cavity is not known. With appropriate boundary conditions, the pressure is given by

$$p = \frac{3\mu U}{rC_R^2}(\ell z - z^2)\frac{n\sin\theta}{(1 + n\cos\theta)^3} - (P_S - P_D)\frac{z}{\ell} + P_S \qquad (2)$$

which on integration around the entire bearing gives total load components

$$P_x = 0 \qquad (3)$$

$$P_y = P = \frac{\mu U \ell^3}{2C_R^2}\frac{n\pi}{(1 - n^2)^{3/2}} \qquad (4)$$

resulting in attitude angle

$$\Phi = \tan^{-1}\frac{P_y}{P_x} = \tan^{-1}\infty = 90^\circ$$

Since the actual value of viscosity μ in the

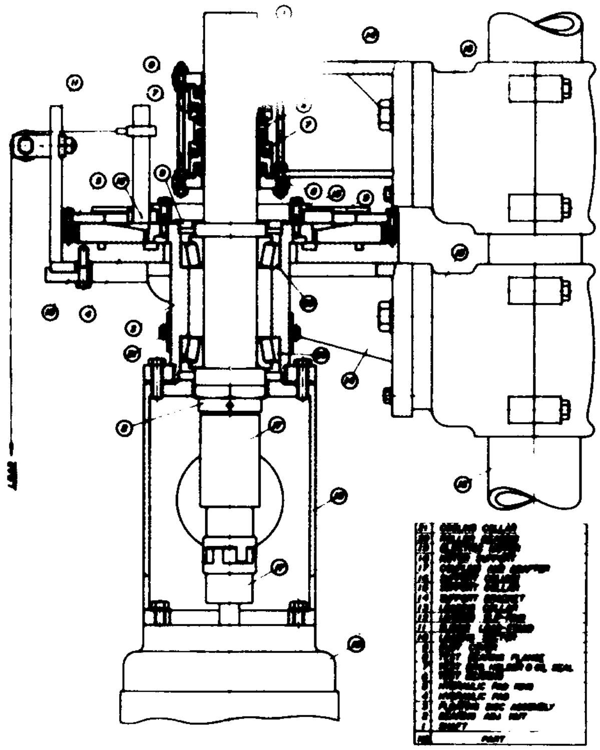

Fig. 2 Section of test apparatus

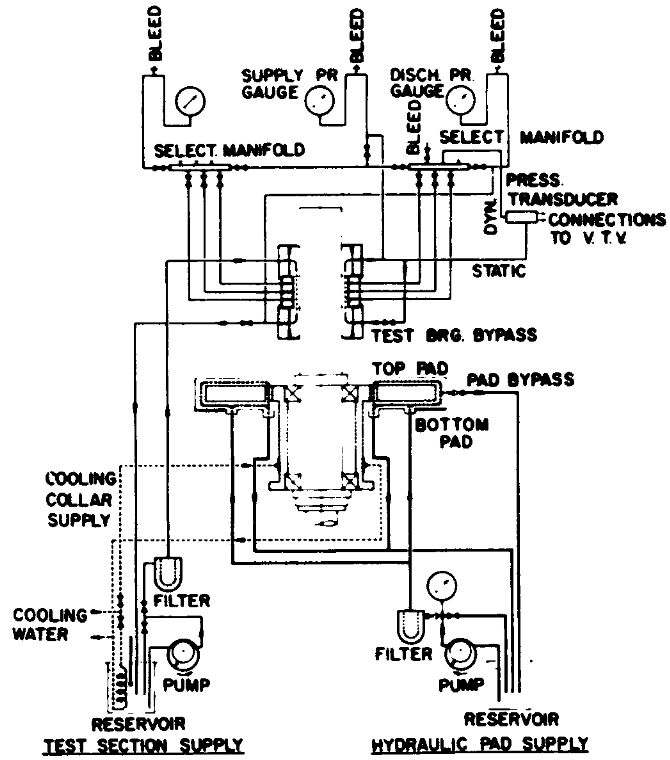

Fig. 3 Instrumentation and service piping diagram

oil film was not known, it was calculated from equation (4) using experimental values for eccentricity ratio n, applied load P and surface speed U. The value of μ thus obtained, was then used to construct theoretical pressure-distribution curves shown by dotted lines in Figs.5 and 6.

The pressure distribution for a case where cavitation was suppressed (no discontinuities in low-pressure region) by the elevated plenum pressures and with a minimum axial gradient is shown in Fig.6. Axial pressure distribution is very nearly symmetric as would be expected on the basis of the theoretical solution. Small discontinuities at the changeover points from one set of pressure taps to the other are consistent for all tests and can be attributed to bearing irregularities. The largest deviation between the theoretical and experimental curves is in the extreme high and low-pressure regions, amounting to about 1.5 psi or less than 4 per cent of the maximum circumferential pressure variation given by the theoretical solution for the middle line of the bearing. Agreement with theory is also very good for the attitude angle ϕ and the angular location of the extreme pressure regions.

Pressure-distribution curves for the 60-lb load and slightly higher axial gradient shown in Fig.7 are of essentially similar shape, only pressure variations are larger due to higher eccentricity ratio. The cavitation is effectively suppressed by the elevated datum pressure except

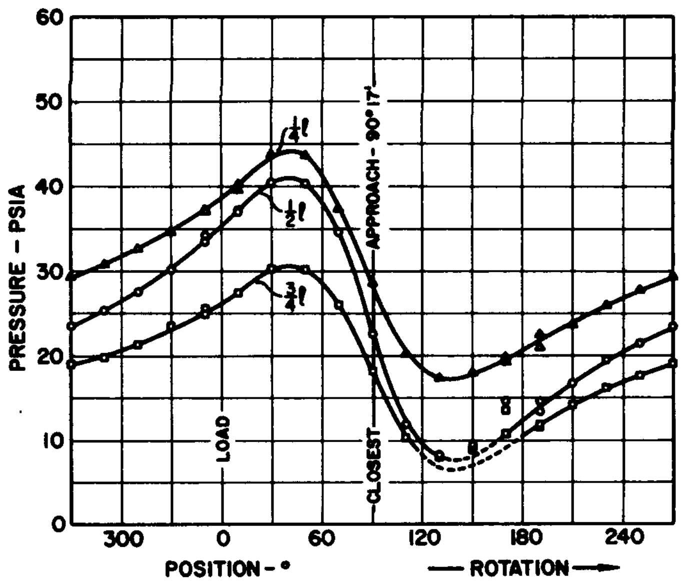

Fig. 4 Test-bearing pressure distribution with 30-lb load and 20 psi/in. axial pressure gradient

Supply pr = 20 psig	RPM = 3490
Disch. pr = 0 psig	n = 0.357
μ = 5.05 cpoise	d = 2 in. ℓ = 1 in.
Temp = 73 $\pm$ 3°F	C_R = 0.00205

for a small extreme low-pressure region near the middle.

The effects of increasing the axial pressure

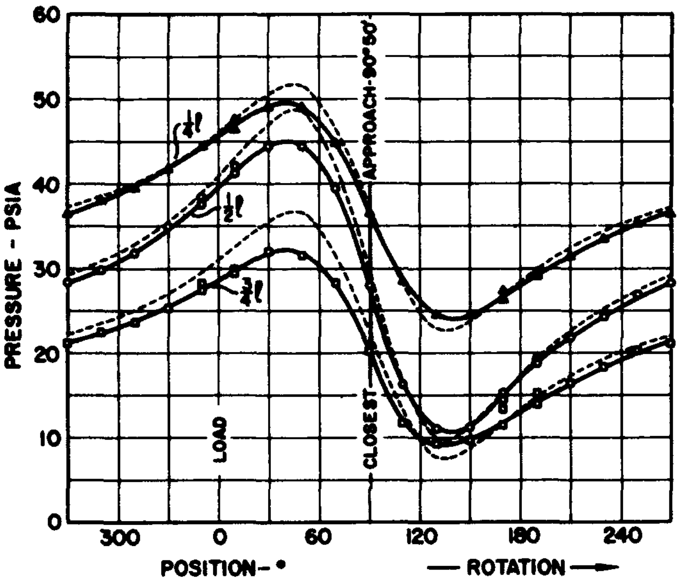

Fig. 5 Test-bearing pressure distribution with 30-lb load and 30 psi/in. axial pressure gradient

Supply pr = 30 psig	RPM = 3480
Disch. pr = 0 psig	n = 0.337
μ = 4.81 cpoise	calc. μ = 3.71 cpoise
Temp = 76.5 $\pm$ 1.5 °F	D = 2 in. ℓ = 1 in.
	C_R = 0.00205

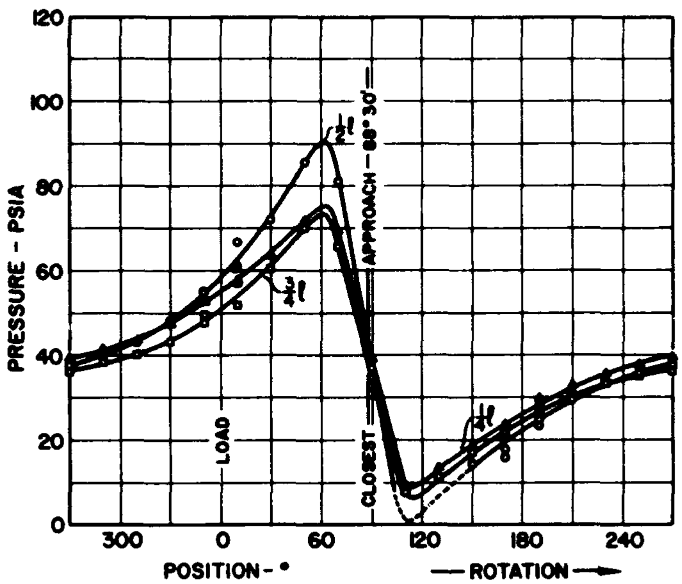

Fig. 7 Test-bearing pressure distribution with 60-lb load, 5 psi/in. axial pressure gradient and 25 psig supply

Supply pr = 25 psig	RPM = 3480
Disch. = 19.95 psig	n = 0.575
μ = 4.66 cpoise	d = 2 in. ℓ = 1 in.
Temp = 78.5 $\pm$ 1.5 °F	C_R = 0.00205

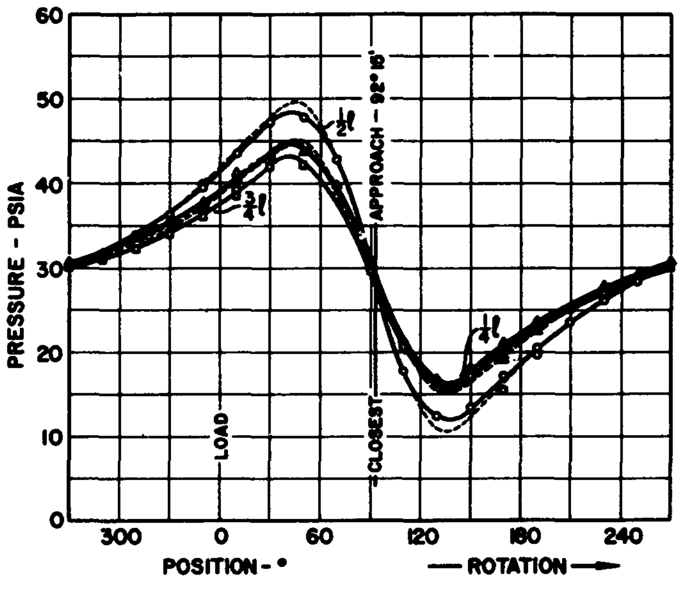

Fig. 6 Test-bearing pressure distribution with 30-lb load, 1 psi/in. axial pressure gradient and 16 psig supply

Supply pr = 16 psig	RPM = 3480
Disch. pr = 15 psig	n = 0.338
μ = 4.90 cpoise	calc μ = 3.71 cpoise
Temp = 75.0 $\pm$ 1.0 °F	d = 2 in. ℓ = 1 in.
	C_R = 0.00205

Fig. 8 Cavitation in journal-bearing oil film

Load = 60 lb	n = 0.624
Speed = 3530 rpm	Φ = 76°45'
P_S = 4.3 psig	Supply, μ = 4.83 cpoise
P_D = 0 psig	Extent of cavity 90 to 350 deg
Cavity shape is stable	

gradient appear in Figs. 4 and 5. In general, the pressure distribution at any one station ($1/4\ell$, $1/2\ell$, and $3/4\ell$ from supply plenum) is unaffected by the axial gradient; the curves are merely shifted to different datum pressure levels. However, additional tests show that there is a slight but consistent tendency for corresponding curves to become more peaked as the axial pressure gradient increases. The implication is: With low axial pressure gradients, axial flow reversal takes place and pressure peaks tend to be suppressed (since there is little or no supply from the low-pressure discharge side); while with high

Fig. 9 Cavitation in journal-bearing oil film

Load = 60 lb; $n = 0.576$
Speed = 3530 rpm; $\Phi = 82^\circ 52'$
P_S = 6.5 psig; Supply μ = 4.83 cpoise
P_D = 0 psig; Extent of cavity 100 to 340 deg
Top edge of cavity unstable

Fig. 11 Cavitation in journal-bearing oil film

Load = 60 lb; $n = 0.505$
Speed = 3470; $\Phi = 98.8^\circ$
P_S = 11.8 psig; Supply μ = 4.75 cpoise
P_D = 10 psig; Extent of cavity 130 to 280 deg
Cavity shape is unstable

Fig. 10 Cavitation in journal-bearing oil film

Load = 60 lb; $n = 0.502$
Speed = 3510 rpm; $\Phi = 94^\circ 5'$
P_S = 10 psig; Supply μ = 4.90 cpoise
P_D = 0 psig; Extent of cavity 130 to 290 deg
Partly unstable

Fig. 12 Cavitation in journal-bearing oil film

Load = 60 lb; $n = 0.47$
Speed = 3456; $\Phi = 98^\circ 40'$
P_S = 14.3 psig; Supply μ = 4.70 cpoise
P_D = 9.6 psig; Extent of cavity 140 to 280 deg

Cavity is unstable, wanders axially and tail end forms separate bubbles which tend to be carried right through the high-pressure region

axial pressure gradients, axial flow reversal does not occur and distribution curves have a more peaked form.

By increasing the axial pressure gradient, it is possible to force the cavitation region towards the discharge end, and for all practical purposes, suppress it entirely, Fig.5. For such case, the agreement with theory is considerably poorer. At mid-point the difference is 3.0 psi or 10 per cent of the maximum theoretical pressure variation, while at 3/4 axial distance, the respective values are 4.6 psi or 16.7 per cent.

No conclusion can be drawn whether differences are caused by reversals in axial flow directions as discussed in the foregoing or by some other phenomena. Additional experimental data with higher axial gradients may give a clearer indication of the deviation trend.

VISUAL OBSERVATION OF CAVITATION

For cavitation observation, the 2.0000-in-OD shaft was used with a lapped Lucite bearing of 2.0034 in. average ID, 1 in. long and 3/4-in-thick wall to minimize distortion. Radial-clearance variations were less than 6 per cent of the average C_R value of 0.0017 in.

Photographic recording of cavitation phenomena was unexpectedly difficult; floodlight reflections on the polished shaft blanked out large areas by overexposure, and contrast between oil film and cavity was very poor. Reflections were finally eliminated by surrounding the test section with a matte white screen (with peepholes for camera) illuminated by floodlights from above. Contrast was improved by coloring the lubricant with red gasoline dye and photographing through a green filter.

Figs.8 to 15 show typical cavitation behavior in the divergent oil film region at different operating conditions. The stated values of eccentricity ratio n and attitude angle Φ are based on readings with load in one position only. The radial clearance C_R of the installed test bearing was checked by extreme dial-gage readings several times after apparatus warmup and between test runs, and was found to be consistently 0.0014 in., allowing for ±0.00005 gage reading accuracy. The foregoing value was considered to be more correct, and was used in calculations, since it was likely that the Lucite bearing underwent some deformation due to axial stress and temperature change.

All photographs were taken with camera located as shown in Fig.1 and show the divergent part of the oil film. Still photographs were taken at 1/100 sec exposure and motion pictures at 65 frames per sec at 1/250 sec exposure.

With low axial-pressure gradient and atmospheric discharge, Fig.8, the cavity is well defined and stable in shape, but contrary to the usual assumption that it extends only over the theoretical negative pressure region (i. e., 180 deg or less) the circumferential extent of the cavity is about 260 deg. Axially the cavity covers about two thirds of the bearing length at the start and narrows down along the upper edge to about half the bearing length before collapsing. This clearly indicates that the extent of the cavitation region is much larger than expected on the basis of theory. The "effective" high-pressure region supporting the load covers only some 100 deg; however, the attitude angle Φ is still close to the value predicted by Ocvirk's solution.

Increasing the axial-pressure gradient, Fig. 9, results in narrowing of the cavity from the supply side, particularly at the tail end of the cavity, also the leading-edge location becomes unstable (similar but not as pronounced as in Fig.13). The eccentricity ratio n drops, although there is relatively little change in the angular extent of the cavity.

Fig.10 shows a recurring shape in an unstable cavity that took different shapes (resembling those in Fig.14) and tended to jump axially back and forth over the middle portion of the bearing. It is of interest that the attitude angle becomes larger than 90 deg as the angular extent of the cavity approaches half the circumference of the bearing; this is in good agreement with results obtained during pressure-distribution measurements.

With low axial-pressure gradients, but elevated plenum pressures, cavities are localized near the middle of the bearing, they are somewhat more stable, and considerably smaller unstable cavities can be observed, Figs.11 and 15. Of particular interest is the unstable cavitation shown in Fig.12. In this case, the tail end of the cavity does not collapse uniformly as in all other cases with larger size cavities; instead, the cavity narrows down and breaks up into separate bubbles which tend to penetrate deep into the high-pressure region before they collapse. Occasionally small bubbles fail to collapse even in the high-pressure region and are carried through into

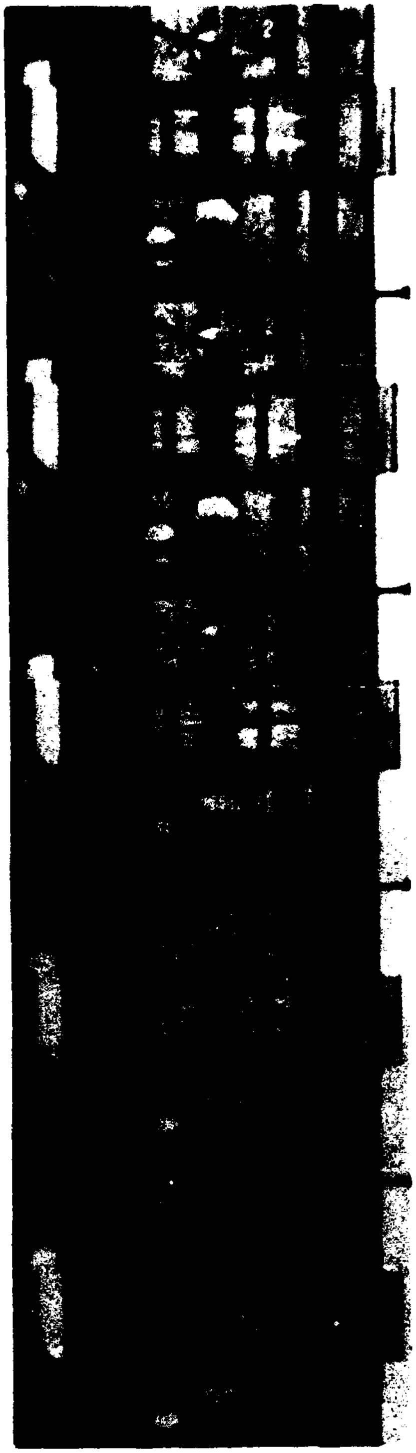

Fig. 13 Cavitation in journal-bearing oil film

Load = 60 lb   n = 0.505
Speed = 3510 rpm Φ = 98°8'
P_S = 7.8 psig   Supply μ = 5.08 cpoise
P_D = 0 psig
64 frames per sec at 1/250 sec

Fig. 14 Cavitation in journal-bearing oil film

Load = 60 lb n = 0.47
Speed = 3420 rpm Φ = 98°40'
P_S = 8.7 psig Supply μ = 5.08 cpoise
P_D = 0 psig

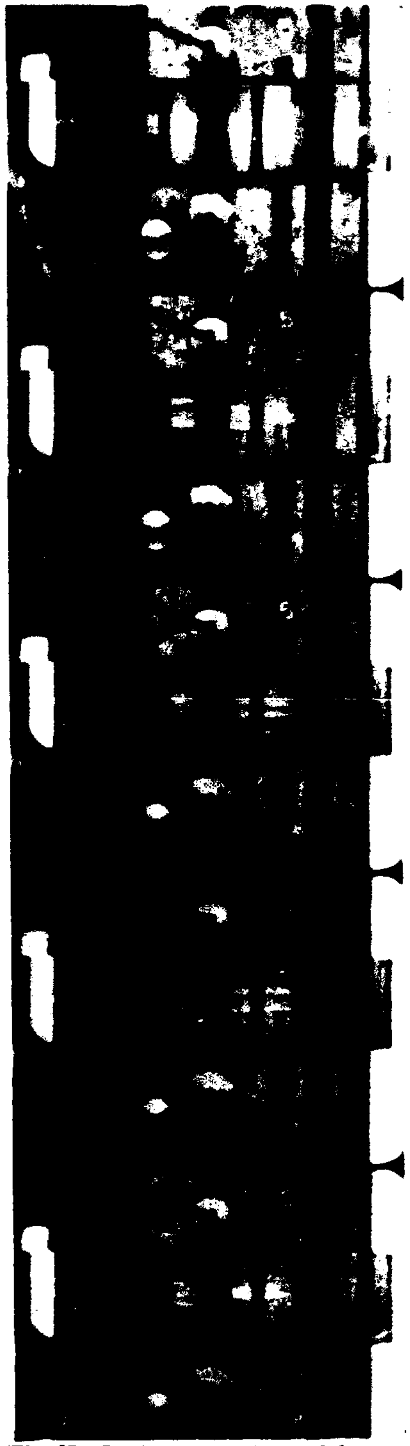

Fig. 15 Cavitation in journal-bearing oil film

Load = 60 lb n = 0.435
Speed = 3440 rpm Φ = 99°25'
P_S = 10.8 psig Supply μ = 4.91 cpoise
P_D = 9.5 psig

the low-pressure region where they initiate a new cavity. The paths of such bubbles are indicated by arrows in Fig.12 and in the third and fourth frames of Fig.14. Further study of this phenomenon could pro·ide information for explaining fatigue failures in bearing surfaces.

One additional phenomenon was observed in the tail-end region of large cavities (not visible on photographs). At the point of cavity collapse, small droplets of lubricant tended to separate and were drawn into the cavity where they slowly drifted in the direction opposite to the journal rotation. This indicates a pressure gradient within the cavity in the direction opposite to rotation.

CONCLUSION

In short journal bearings operating with a small axial-pressure gradient and low supply pressure, the negative pressure region has the tendency to be relieved as evidenced by discontinuities in the experimental pressure-distribution curves. Visual observations of the oil film have shown conclusively that the mechanism by which negative pressures are relieved is cavitation and not reverse flow as suggested by Wannier's theory. Apparently the oil film is too thin for this theory to be applicable.

The experimental results are in close agreement with Ocvirk's short journal-bearing solution (1) when axial-pressure gradient is low and cavitation is suppressed by pressurizing the bearing. On the other hand, when cavitation is suppressed only by elevated supply pressure resulting in high axial gradient, appreciable differences exist between experimental and theoretical pressure distributions, while for attitude angle the agreement is still very close. Thus, in engineering applications, load-carrying capacity can be doubled at the same eccentricity ratio by pressurization and for low axial gradients, the necessary pressures can be determined from Ocvirk's solution without appreciable error. For more common applications where the load-carrying capacity would be increased by suppressing cavitation only with increased supply pressure, the foregoing solution appears inadequate unless the theory can be corrected for the cavitation region and for the effect that a high axial-pressure gradient has on the pressure distribution.

Visual observation shows that although cavitation is primarily governed by datum pressure and/or axial-pressure gradient, the shape and location of the cavity are strongly influenced by the defects and roughness of the bearing and journal surfaces. Isolated bubbles form and penetrate deeply into the high-pressure region when cavitation is highly unstable; a phenomenon which may have considerable significance in explaining bearing material fatigue failures.

ACKNOWLEDGMENTS

The author is indebted to Prof. A. J. Acosta for his guidance and contributions during the course of this investigation. He also wisnes to thank Prof. D. S. Wood for his assistance in solving the engineering problems encountered during the apparatus design and Mr. C. T. Eastvedt for his advice and assistance in photographic recording of the cavitation phenomena.

REFERENCES

1 G. B. Dubois and F. W. Ocvirk, "Analytical Derivation and Experimental Evaluation of Short-Bearing Approximation for Full Journal Bearings," NACA 1157, 1953.

2 S. A. McKee and T. R. McKee, "Pressure Distribution in Oilfilms of Journal Bearings," Trans. ASME, vol. 54, 1932, pp. 149-165.

3 J. A. Cole, "Low Pressure Regions Occurring in the Hydrodynamic Films of Journal Bearings," Scientific Lubrication, vol. 3, 1951, p. 10.

4 G. Wannier, "A Contribution to the Hydrodynamics of Lubrication," Quarterly of Applied Mathematics, vol. 8, 1950, pp. 1-32.

5 M. J. Jacobson, A. Charnes, and E. Saibel, "The Complete Journal Bearing with Circumferential Oil Inlet," Trans. ASME, vol. 77, 1955, pp. 1179-1183.

6 D. Dawson, "Investigation of Cavitation in Lubricating Films Supporting Small Loads," IME Conference on Lubrication and Wear, Paper No. 49, October 1957.

7 J. A. Cole and C. J. Huges, "Visual Study of Film Extent in Dynamically Loaded Complete Journal Bearings," IME Conference on Lubrication and Wear, Paper No. 87, October 1957.